

Study of the Glycerol Hydrogenolysis Reaction on Cu, Cu–Zn, and Cu–ZnO Clusters

Ram Singh, Prakash Biswas, and Prateek K. Jha*

Cite This: *ACS Omega* 2022, 7, 33629–33636

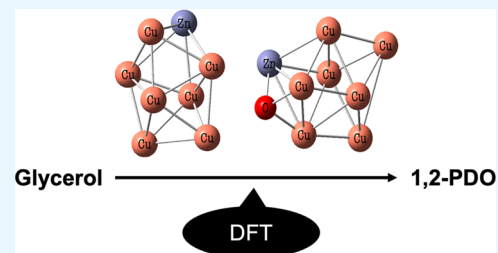
Read Online

ACCESS |

Metrics & More

Article Recommendations

ABSTRACT: Quantum chemistry calculations have been performed to access the efficacy of Cu-based catalysts in various mechanistic steps of the glycerol hydrogenolysis reaction. Calculations are first performed for reactants in the gas phase (noncatalyzed system) and reactants in the gas phase with a 3-atom Cu cluster (catalyzed system). We demonstrate that the glycerol to ethylene glycol conversion is preferred in the noncatalyzed system but glycerol conversion to 1,2-propanediol via the 2-acetol intermediate is preferred in the catalyzed system. We next analyze the adsorption energies of the reactant and product species involved in the glycerol to 1,2-PDO reaction on an 8-atom Cu cluster and Cu cluster doped with a Zn atom or a ZnO molecule. Finally, we study the effects of Zn or ZnO doping on the activation barriers of the two steps of the glycerol to 1,2-PDO reaction.



1. INTRODUCTION

Glycerol conversion to value-added products has received significant scientific attention in recent years. One of the main motivating forces for this trend is the fact that glycerol (propane-1,2,3-triol) is produced in large quantities during biodiesel production,^{1,2} that is, roughly 10% by weight of the produced biodiesel. Two of the most useful value-added products of glycerol are 1,2-propanediol (1,2-PDO) and 1,3-propanediol (1,3-PDO),³ which are formed by the hydrogenolysis of glycerol. From a mechanistic perspective, PDO formation requires the use of catalysts that facilitate the formation of a C=O bond, which is otherwise less favored than the formation of a C=C bond. Several transition metal and noble metal catalysts^{4–7} have been tried over the years for the hydrogenolysis reaction, which exhibit various degrees of selectivity to the formation of 1,2-PDO and 1,3-PDO. In general, while 1,3-PDO is considered more valuable than 1,2-PDO, the latter is generally the dominant product of the hydrogenolysis reaction.⁸ 1,2-PDO finds use in the manufacturing of unsaturated polyester resins, paints, and cosmetics and as starting materials in printing, pharmaceuticals, etc.^{3,9,10}

The actual mechanism of the glycerol hydrogenolysis reaction is debated, and several possible reaction schemes have been proposed.⁹ Figure 1 shows probably the most accepted scheme showing the common products of the hydrogenolysis reaction. The formation of PDO from glycerol (I) proceeds via an acetol intermediate, which involves the cleavage of the C–OH bond to form a C=O bond. Depending on which C–OH bond is attacked, 2-acetol (II) or 1-acetol (III) can be formed, which may then be hydrogenated to form 1,2-PDO (IV) or 1,3-PDO (V), respectively. In principle, IV and V may further hydrogenolyze

to form the over-hydrogenolysis products, 2-propanol (VI) and 1-propanol (VII), respectively. As an alternative to the formation of the acetol intermediate, the hydrogenolysis reaction may also result in the formation of ethylene glycol (VIII) by cleavage of the C–C bond, followed by its subsequent hydrogenolysis to ethanol (IX). IX and methanol (X) may also be formed by the hydrogenation of PDO. Taking into consideration all the above-mentioned possible reactions, one should use catalysts that facilitate the cleavage of the C–OH bond without attacking the C–C bond of the glycerol molecule, to have higher selectivity toward PDO. Moreover, the formation of IX and X needs to be suppressed by selection of appropriate reaction conditions. As an alternate to the mechanism proposed in Figure 1, the formation of 1,2-PDO by hydrogenolysis may also occur by glycerol dehydrogenation to glyceraldehyde followed by its dehydration and hydrogenation to 1,2-PDO or a “direct” glycerol hydrogenolysis.⁹ In this paper, we are interested in Cu-based catalysts, in which the formation of PDO via an acetol intermediate has been established in several experimental studies.^{4–6,11,12}

Recently, Pandey et al.¹⁴ have investigated the use of different acid- and base-supported Cu–Zn bimetallic catalysts for glycerol hydrogenolysis in the vapor phase, in which Cu–Zn/MgO was found to be most selective to 1,2-PDO and

Received: August 19, 2022

Accepted: August 26, 2022

Published: September 7, 2022



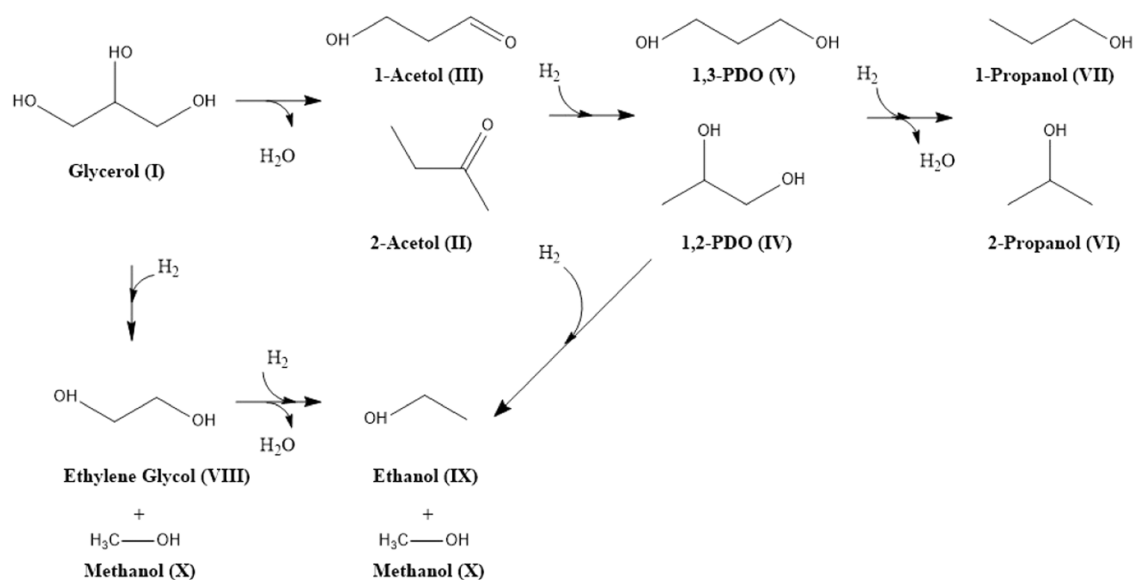


Figure 1. Reaction mechanism for selective glycerol hydrogenolysis.¹³ Adapted with permission from “Production of 1,2-Propanediol from Renewable Glycerol Over Highly Stable and Efficient Cu–Zn(4:1)/MgO Catalyst”, *Catalysis Letters* (Springer Nature), 147, 2783–2798 (2017).

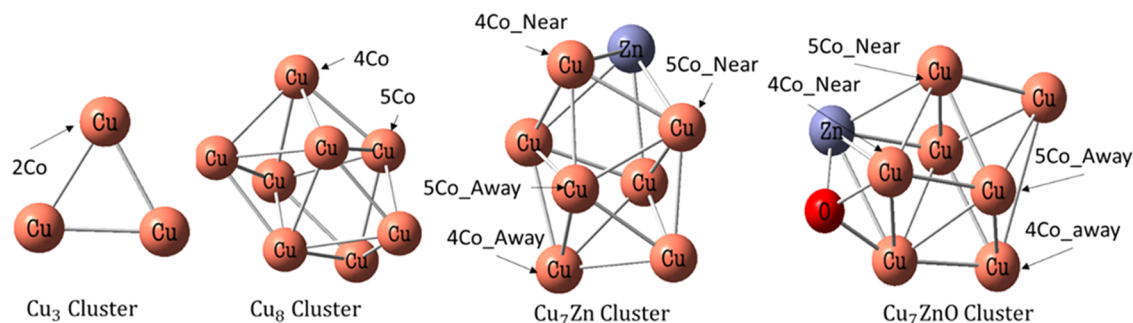


Figure 2. Schematic of different clusters used in this work and representation of different types of Cu sites on these clusters. $x\text{Co}$ ($x = 2, 4, 5$) indicates a Cu atom with x bonded neighbors, i.e., coordination number x . For clusters containing Zn atoms, “_Near” or “_Away” is suffixed to indicate Cu atoms bonded to or away from Zn atom, respectively.

resulted in almost 100% conversion. Mondal et al.¹³ have also reported nearly 100% conversion with 94% selectivity to 1,2-PDO with the Cu–Zn(4:1)/MgO catalyst in the liquid phase. They attributed the increased performance to a “hydrogen spillover” effect, which is the migration of the hydrogen atoms from the metal catalyst onto the nonmetal supports. Hydrogen spillover may increase the reducibility of the Cu catalyst, thus increasing the reaction selectivity toward 1,2-PDO. A similar finding was also reported in a study by Xia et al.,¹⁵ using different compositions of Cu_{0.4}/Zn_{5.6–x}Mg_xAl₂O_{8.6} catalysts for the hydrogenolysis of glycerol reaction. Interestingly, some researchers have reported that ZnO (acidic site) shows activity for glycerol dehydration to acetol and hydrogenation occurs on Cu sites.^{10,16} Zhou et al.¹⁷ performed a kinetic study on glycerol hydrogenolysis to 1,2-PDO over the Cu–ZnO–Al₂O₃ catalyst and concluded that dehydration–hydrogenation through acetol is the preferred route. They have also determined the activation barriers for dehydration and hydrogenation reactions as 86.56 and 57.80 kJ/mol, respectively.

Although experimental studies have provided many insights into the reaction pathways, theoretical analysis using complementary tools may provide better interpretation at the molecular level. Hirunsit et al.¹⁸ have performed theoretical

and experimental studies on glycerol hydrogenolysis over Cu/Al₂O₃ that showed selectivity for 1,2-PDO. Using density functional theory (DFT) calculations, they have demonstrated that the improved catalytic activity on Cu/Al₂O₃ compared to that of pure Cu results from the presence of acidic Al sites. The mechanisms of glycerol dehydration have been studied by Nimlos et al.¹⁹ using quantum chemistry calculations (using CBS-QB3). They determined the activation barriers to 1,2-dehydration and for pericyclic 1,3-dehydration. Geng et al.²⁰ described four possible routes of glycerol pyrolysis using quantum chemistry calculations and investigated the energy barriers and reaction rate constants to analyze the possible pyrolysis mechanisms. Laino et al.²¹ investigated the dehydration mechanism of glycerol in the gas phase and showed that the glycidol barrier is 66.8 kcal/mol, which is the rate-limiting step of glycerol decomposition. More recently, Karim et al.²² described the water dissociation and dehydrogenation of glycerol over Au(111) and PdAu alloy catalyst surfaces to produce hydrogen. Guan et al.²³ have performed thermodynamic analysis of glycerol hydrogenolysis to propanediols over supported Cu clusters using periodic density functional theory. They reported that Cu/MgO exhibits better activity than that of Cu/ZrO₂ and also shows selectivity to 1,2-PDO in comparison to 1,3-PDO. Chen et

al.²⁴ showed an efficient reaction pathway for glycerol to synthesis gas using C–C bond scission.

This study is the extension of our previous study,²⁵ wherein we performed DFT calculations to study the structure and stability of Cu, Cu–Zn, and Cu–ZnO clusters and adsorption of glycerol and hydrogen on each and every possible coordination of these clusters. In this study, we shift our focus to the hydrogenolysis reaction and first establish that the hydrogenolysis to PDO indeed follows the formation of an acetol intermediate when using a Cu₃ cluster, unlike a noncatalyzed system where ethylene glycol formation is preferred. Next, we study the adsorption energies of reactants and products, activation barriers, rate constants, and reaction energies on each possible coordination site of Cu and Zn atoms in Cu₈, Cu₇Zn, and Cu₇ZnO for the glycerol to 1,2-PDO reaction via the 2-acetol intermediate. The current study together with our previous study²⁵ thus provides useful molecular insights into the use of Cu–Zn and Cu–ZnO catalysts for the glycerol hydrogenolysis reaction.

2. COMPUTATIONAL DETAILS

DFT calculations are carried out using Gaussian 09 software²⁶ with the Gauss View 5 user interface. Optimized geometries are obtained by DFT calculations performed using the B3LYP²⁷ functional combined with the double- ζ -type LanL2DZ^{28–30} basis set, which has been validated and used successfully in our previous study.²⁵ Minimum energy geometries of catalyst clusters (Figure 2), reactants and products, reactants and products adsorbed on catalyst clusters, and transition states of reactions are obtained using optimization calculations. Doublet spin multiplicity is chosen for Cu₃, Cu₇Zn, and Cu₇ZnO clusters having one unpaired electron, and singlet spin multiplicity is chosen for the Cu₈ cluster having no unpaired electrons. The initial assumptions for these calculations are computed by optimization performed using Hartree-Fock(HF)/LanL2DZ theory, which are then reoptimized using B3LYP/LanL2DZ. Energies and vibrational frequencies are then computed for these optimized geometries. No imaginary vibration frequencies are obtained for the minimum energy configurations except for the transition states. Transition states are characterized as having only one imaginary vibrational frequency. Separately, intrinsic reaction coordinate (IRC)³¹ calculations are also performed to confirm the obtained transition states. The activation barriers for reactions shown in Figure 3 are computed as the difference between the energies of the transition state and the reactants. The adsorption energy of a species (“adsorbate”) on a catalyst cluster is computed by the following equation, as used in our previous study.²⁵

$$E_{\text{ad}} = E_{\text{cl-ad}} - E_{\text{cl}} - E_{\text{ad}} \quad (1)$$

where $E_{\text{cl-ad}}$ is the energy of the cluster with the adsorbate (reactant, transition states, products) and E_{cl} and E_{ad} are the individual energies of the cluster and adsorbate, respectively. The reaction rate constants (k) are calculated using transition state theory^{32,33} as

$$k = \frac{k_{\text{B}}T}{h} \exp\left(\frac{-\Delta G^{\ddagger}}{RT}\right) \quad (2)$$

where k_{B} is the Boltzmann constant, h is the Planck constant, R is the gas constant, and ΔG^{\ddagger} is the Gibbs free energy of activation at temperature $T = 298.15$ K. ΔG^{\ddagger} is calculated as

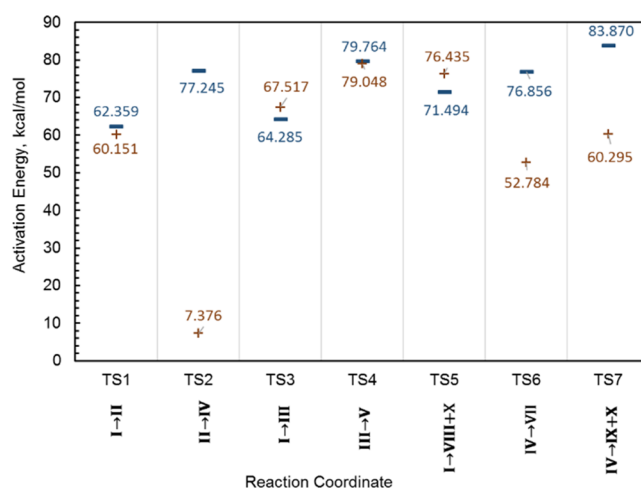


Figure 3. Activation barriers of the reaction mechanism for glycerol hydrogenolysis with a Cu₃ cluster (orange, +) and without a cluster (blue, —).

the difference between the Gibbs free energy of the transition state and the reactant(s). The reaction energy is calculated as the difference of electronic energy (with zero-point correction) between products and reactants. Note that the energies of clusters on which the reactant(s)/product(s) are adsorbed are also included for the purpose of calculation of reaction energy and free energy differences.

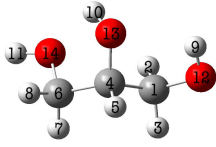

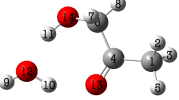
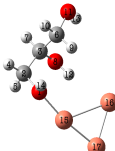
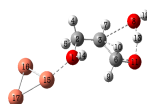
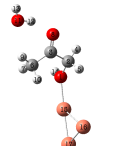
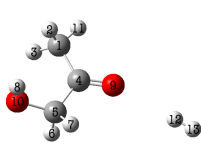
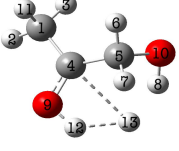
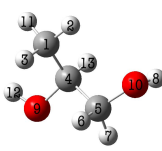
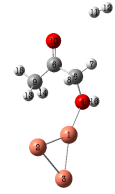
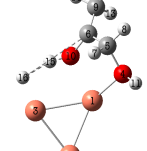
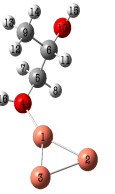
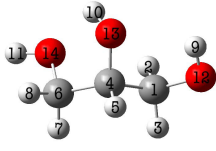
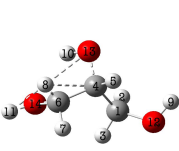
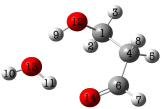
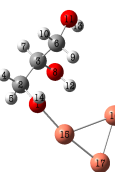
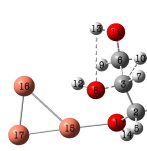
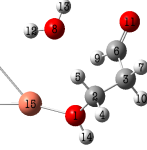
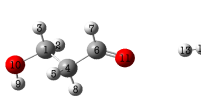
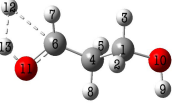
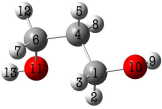
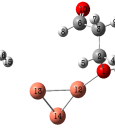
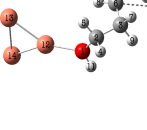
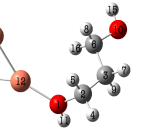
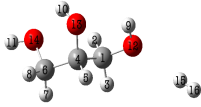

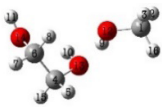
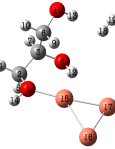
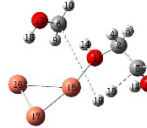
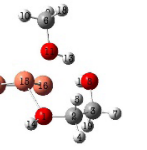
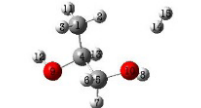
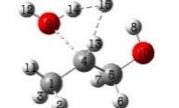
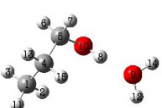
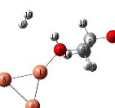
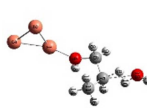
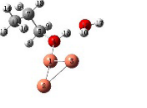
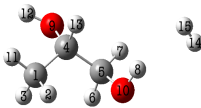
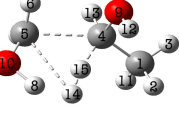
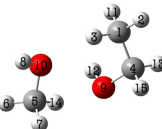
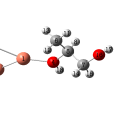
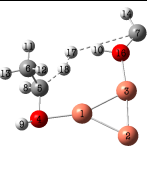
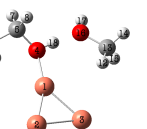
3. RESULTS AND DISCUSSION

3.1. Reaction Mechanism with and without Catalyst Clusters.

The reaction mechanisms of glycerol hydrogenolysis are first studied for the system without and with a Cu₃ cluster. Figure 3 shows the activation barriers for each of the reactions defined as the difference in the energy of the transition state and the reactant(s). The minimum energy geometries of the reactant(s), transition state (TS), and product(s) of the reactions are shown in Table 1, along with their first harmonic frequency. The activation barrier is lowered for all reactions with the use of a Cu₃ cluster except reactions I (glycerol) to III (1-acetol) and I to VIII (ethylene glycol) and X (methanol). Although the activation barrier for the reaction I to II (2-acetol) undergoes a minor reduction (≈ 2.2 kcal/mol) with the use of the Cu₃ cluster, the activation barrier of the subsequent reaction II to IV (1,2-PDO) undergoes a drastic reduction (activation barrier difference of ≈ 69.9 kcal/mol) with the use of the Cu₃ cluster. In contrast, the activation barrier for the conversion of I to VIII and X undergoes an increase with the use of the Cu₃ cluster, and its magnitude (76.435 kcal/mol) is much larger than that of I to II (60.151 kcal/mol) and I to III (67.517 kcal/mol). It is therefore obvious that the a Cu catalyst is highly selective to 1,2-PDO via 2-acetol as established in experimental studies.^{13,18} Also, Cu plays a dominant role in the second conversion step, i.e., 2-acetol (II) to 1,2-PDO (IV). While the conversion of I to II has a lower activation barrier than that of II to IV without a Cu₃ cluster, the latter reaction has a much lower activation barrier when a Cu₃ cluster is used.

Our results for the noncatalyzed system are in reasonable agreement with those of a previous study of Nimlos et al.¹⁹ who have obtained the activation barriers of neutral glycerol dehydration as 70.9 kcal/mol for 1,2-dehydration and 65.2 kcal/mol for 1,3-dehydration. Unlike their case, we have

Table 1. Structures of the Reactant(s), Product(s), and Transition State and Their Respective First Harmonic Frequency Which is Involved in the Glycerol Hydrogenolysis Mechanism

Without Catalyst			With Cu ₃ Cluster		
Reactant(s)	Transition State	Product(s)	Reactant(s)	Transition State	Product(s)
 I 104.90 cm ⁻¹	 TS1 -614.28 cm ⁻¹	 II + Water 72.92 cm ⁻¹	 I 8.34 cm ⁻¹	 TS1 -104.32 cm ⁻¹	 II + Water 8.21 cm ⁻¹
 II + Hydrogen 16.44 cm ⁻¹	 TS2 -750.65 cm ⁻¹	 IV 119.57 cm ⁻¹	 II + Hydrogen 14.25 cm ⁻¹	 TS2 -39.61 cm ⁻¹	 IV 4.77 cm ⁻¹
 I 104.90 cm ⁻¹	 TS3 -408.42 cm ⁻¹	 III + Water 79.07 cm ⁻¹	 I 8.34 cm ⁻¹	 TS3 -986.74 cm ⁻¹	 III + Water 4.06 cm ⁻¹
 III + Hydrogen 16.19 cm ⁻¹	 TS4 -1578.59 cm ⁻¹	 V 90.60 cm ⁻¹	 III + Hydrogen 16.99 cm ⁻¹	 TS4 -20.56 cm ⁻¹	 V 13.78 cm ⁻¹
 I + Hydrogen 9.18 cm ⁻¹	 TS5 -1806.53 cm ⁻¹	 VIII+X 38.02 cm ⁻¹	 I + Hydrogen 7.47 cm ⁻¹	 TS5 -422.10 cm ⁻¹	 VIII+X 8.18 cm ⁻¹
 IV + Hydrogen 29.13 cm ⁻¹	 TS6 -550.76 cm ⁻¹	 VII + Water 38.02 cm ⁻¹	 IV + Hydrogen 12.07 cm ⁻¹	 TS6 -2450.01 cm ⁻¹	 VII + Water 21.58 cm ⁻¹
 IV + Hydrogen 17.45 cm ⁻¹	 TS7 -1779.48 cm ⁻¹	 IX + X 37.45 cm ⁻¹	 IV + Hydrogen 12.07 cm ⁻¹	 TS7 -968.32 cm ⁻¹	 IX + X 7.93 cm ⁻¹

considered a two-step reaction via an acetol intermediate. For 1,2 dehydration without a catalyst, we have obtained the

activation barriers for I to II and II to IV as 62.359 and 77.245 kcal/mol, respectively. Similarly, for 1,3-dehydration without a

Table 2. Adsorption Energy of the Components Involved in the Glycerol Hydrogenolysis Reaction at Every Possible Coordination Site of Cu₈, Cu₇Zn, and Cu₇ZnO Clusters^a

cluster	coordination	E_{Ad} (kcal/mol)				
		glycerol (I)	2-acetol (II)	1,2-PDO (IV)	water	hydrogen
Cu ₈	4Co (4)	-13.854	-13.695	-15.472	-8.639	-0.439
	5Co (4)	-15.962	-9.062	-10.792	-4.670	-0.370
	average over Cu atoms	-14.908	-11.379	-13.132	-6.655	-0.405
Cu ₇ Zn	4Co_near (1)	-13.528	-18.123	-14.780	-0.829	-0.303
	4Co_away (2)	-14.615	-14.351	-16.101	-5.765	-0.061
	5Co_near (3)	-9.755	-10.811	-12.244	-4.792	0.102
	5Co_away (1)	-12.151	-11.642	-12.783	-3.983	-0.275
	average over Cu atoms	-12.025	-12.986	-13.785	-4.388	-0.056
	Zn	-7.032	-7.737	-12.538	-2.666	-0.092
Cu ₇ ZnO	average over Cu and Zn atoms	-11.401	-12.330	-13.629	-4.173	-0.061
	4Co_near (1)	-15.406	-17.188	-19.646	-5.221	0.139
	4Co_away (2)	-16.099	-15.540	-15.617	0.599	1.702
	5Co_near (3)	-13.782	-19.829	-14.957	-0.704	4.629
	5Co_away (1)	-16.107	-15.350	-15.402	2.753	-0.265
	average over Cu atoms	-15.008	-17.586	-15.879	-0.483	2.452
	Zn	-30.487	-19.869	-29.318	-1.674	0.062
	average over Cu and Zn atoms	-16.943	-17.872	-17.559	-0.632	2.153

^aValues given in the bracket are the number of particular sites available in the clusters. Average values are computed using the number of coordination sites (given in brackets) as weights.

catalyst, the activation barriers for I to III and III to V are obtained as 64.285 and 79.764 kcal/mol values, respectively.

With regard to the over-hydrogenolysis products of IV in the presence of the Cu₃ cluster, the conversion of IV to VII has a lower activation barrier (52.784 kcal/mol) compared to the conversion of IV to IX+X (60.295 kcal/mol). This is also observed without a Cu₃ cluster, where the latter reaction has an activation barrier (83.870 kcal/mol) higher than that of the former reaction (76.856 kcal/mol). Note that the activation barrier for the formation of 2-propanol (VI) from 1,2-PDO (IV) is 76.974 kcal/mol with a cluster and 83.461 kcal/mol without a cluster, both of which is higher than that of the 1-propanol (VII) case reported in Figure 3. Thus, it can be concluded that VII is the most preferred over-hydrogenolysis product of glycerol.

In the following, we study the conversion of I to IV via II in more detail. Minimum energy 8-atom clusters, Cu₈, Cu₇Zn, and Cu₇ZnO, are taken from our previous study.²⁵ This cluster size is selected because of the existence of a three-dimensional (3D) structure and availability of several types of coordination sites. In Section 3.2, we discuss the study of the adsorption of the reactants and products of these reactions. This is followed by a discussion of the activation barriers, reaction energy, and rate constants in Section 3.3.

3.2. Adsorption of Species. The adsorption energies of the reactants and products (Table 2) are calculated using eq 1 at every possible coordination site of 8-atom clusters as shown in Figure 2. The adsorbed structures of the reactants, products, and transition states are given in Table 3. It can be inferred from Table 3 that the hydrogen molecule does not get adsorbed or weakly adsorbed on the cluster site during the reaction as also found in our previous study,²⁵ but it stays near the cluster. Similarly, the water molecule is also not adsorbed or weakly adsorbed on the cluster surface but stays near the cluster. These are reflected in the less negative values of adsorption energy for hydrogen and water molecules in Table 2. It may therefore be concluded that the hydrogen and water molecules are in the gas phase during the hydrogenolysis

reaction, and the species having more negative adsorption energy values, i.e., glycerol (I), 2-acetol (II), and 1,2-PDO (IV), are adsorbed on the cluster. In particular, the average adsorption energies of hydrogen and water molecules over all Cu and Zn atoms are the least negative for the Cu₇ZnO cluster.

For the Cu₈ cluster, more negative adsorption energy is obtained for I on the 5Co site (-15.962 kcal/mol). In contrast, more negative adsorption energies for II and IV are obtained for the 4Co site, which are -13.695 and -15.472 kcal/mol, respectively. After Zn doping, i.e., for the Cu₇Zn cluster, the most negative adsorption energies are obtained for I and IV on the 4Co_Away site and for II on the 4Co_Near site. This implies that the presence of Zn on the neighboring site favors adsorption of II on the Cu atom but not the adsorption of I and IV. In the case of the Cu₇ZnO cluster, the adsorption energies of I, II, and IV are most negative on the Zn atom, which implies that ZnO doping facilitates stronger adsorption of species. The same can be inferred by looking at the average adsorption energy over Cu and Zn atoms for all clusters, which is most negative for the Cu₇ZnO cluster. Also, if the adsorption energy is averaged only over Cu atoms in the cluster, adsorption energies are still most negative for the Cu₇ZnO cluster, implying that ZnO doping facilitates increased adsorption on Cu sites as well. In our earlier study,²⁵ we have already established an increase in the physical stability of Cu clusters with ZnO doping.

3.3. Activation Barriers, Reaction Energy, and Rate Constant. Table 4 shows the activation barriers, rate constants, and reaction energies of I to II + water (via TS1) and II + hydrogen to IV (via TS2) without a catalyst and with Cu₈, Cu₇Zn, and Cu₇ZnO clusters at every possible coordination sites. Some of the values (indicated by *) in Table 4 could not be computed using B3LYP/LanL2DZ theory despite repeated trials, and therefore, values computed using HF/LanL2DZ theory are shown for these cases. Activation barriers (E_a) are calculated as the differences of the transition state energy (TS1, TS2) and the respective

Table 3. Structures of Reactants, Products, and Transition States and Their Respective First Harmonic Frequency for the Species Involved in the Glycerol Hydrogenolysis Mechanism Over Cu₈, Cu₇Zn, and Cu₇ZnO Clusters at Every Possible Coordination Sites

Cluster	Coordination	Glycerol (I)	TS1	2-Acetol (II)+ Water	2-Acetol (II) + Hydrogen	TS2	1,2-PDO (IV)
Cu ₈	4Co	 12.71 cm ⁻¹	 -494.12 cm ⁻¹	 20.99 cm ⁻¹	 5.63 cm ⁻¹	 -1352.39 cm ⁻¹	 5.04 cm ⁻¹
	5Co	 9.13 cm ⁻¹	 -31.37 cm ⁻¹	 7.94 cm ⁻¹	 7.36 cm ⁻¹	 -845.67 cm ⁻¹	 9.94 cm ⁻¹
Cu ₇ Zn	4Co_Near	 11.56 cm ⁻¹	 -204.47 cm ⁻¹	 9.62 cm ⁻¹	 4.93 cm ⁻¹	 -26.23 cm ⁻¹	 8.96 cm ⁻¹
	4Co_Away	 9.14 cm ⁻¹	 -1791.75 cm ⁻¹	 6.15 cm ⁻¹	 8.59 cm ⁻¹	 -93.42 cm ⁻¹	 4.28 cm ⁻¹
	5Co_Near	 7.56 cm ⁻¹	 -184.56 cm ⁻¹	 9.67 cm ⁻¹	 9.94 cm ⁻¹	 -35.30 cm ⁻¹	 5.75 cm ⁻¹
	5Co_Away	 10.69 cm ⁻¹	 -107.84 cm ⁻¹	 9.72 cm ⁻¹	 11.95 cm ⁻¹	 -83.28 cm ⁻¹	 9.09 cm ⁻¹
	Zn site	 8.84 cm ⁻¹	 -3012.07 cm ⁻¹	 8.74 cm ⁻¹	 7.37 cm ⁻¹	 -145.48 cm ⁻¹	 9.09 cm ⁻¹
Cu ₇ ZnO	4Co_Near	 33.84 cm ⁻¹	 -3050.51 cm ⁻¹	 11.41 cm ⁻¹	 8.74 cm ⁻¹	 -1149.65 cm ⁻¹	 16.27 cm ⁻¹
	4Co_Away	 13.24 cm ⁻¹	 -437.13 cm ⁻¹	 7.72 cm ⁻¹	 12.55 cm ⁻¹	 -1532.59 cm ⁻¹	 12.60 cm ⁻¹
	5Co_Near	 10.67 cm ⁻¹	 -1475.11 cm ⁻¹	 49.22 cm ⁻¹	 12.94 cm ⁻¹	 -665.05 cm ⁻¹	 14.57 cm ⁻¹
	5Co_Away	 13.53 cm ⁻¹	 -2429.28 cm ⁻¹	 29.20 cm ⁻¹	 19.55 cm ⁻¹	 -1002.41 cm ⁻¹	 25.74 cm ⁻¹
	Zn site	 8.23 cm ⁻¹	 -54.05 cm ⁻¹	 13.13 cm ⁻¹	 11.25 cm ⁻¹	 -31.76 cm ⁻¹	 13.52 cm ⁻¹

reactant(s) energy with zero-point energy corrections. Reaction rate constants are calculated using eq 2. Reaction energies are calculated as the differences of the energy of product(s) and reactant(s) of the reactions. Very low rate constants ($\sim 10^{-33} \text{ s}^{-1}$) for I to II + water and $\sim 10^{-47} \text{ s}^{-1}$ for II

+ hydrogen to IV and much higher activation barriers were found for the reaction without the catalyst clusters compared with the reaction with the catalyst clusters, which establishes that the reactions are not feasible without a catalyst. All the reactions are found to be exothermic as implied by the negative

Table 4. Reaction Activation Barrier, Rate Constant, and Reaction Energy of Glycerol Hydrogenolysis over Cu₈, Cu₇Zn, and Cu₇ZnO Clusters at Every Possible Coordination Sites^a

cluster	coordination	E_a (kcal/mol)		rate constant (s^{-1})		RE (kcal/mol)	
		TS1	TS2	k_1 ($\times 10^{12}$)	k_2 ($\times 10^{12}$)	RE ₁	RE ₂
without a catalyst		62.359	77.245	$\sim 10^{-45}$	$\sim 10^{-59}$	-16.268	-13.453
Cu ₈	4Co (4)	33.368	41.215	$\sim 10^{-9}$	$\sim 10^{-11}$	-24.712	-14.517
	5Co (4)	11.185	18.166	6.059	5.950	-14.101	-14.554
	average	22.277	29.691	3.0295	2.975	-19.407	-14.536
Cu ₇ Zn	4Co_near (1)	2.545	16.763	6.178	6.007	-21.252	-9.712
	4Co_away (2)	26.023	70.740	5.921	5.493	-21.163	-14.795
	5Co_near (3)	17.026*	46.163*	6.004	5.703	-21.744	-15.008
	5Co_away (1)	20.828	4.339	5.978	6.092	-19.088	-14.027
	Zn site (1)	38.577*	50.040*	5.778	5.689	-44.322	-24.544
	average over Cu and Zn atoms	20.634	43.889	5.974	5.735	-24.028	-15.362
Cu ₇ ZnO	4Co_near (1)	52.469	69.203	6.021	5.509	-9.736	-23.781
	4Co_away (2)	38.479	40.208	5.800	5.775	-9.170	-17.669
	5Co_near (3)	17.083	42.425	5.953	5.738	-46.481	-19.397
	5Co_away (1)	9.152	26.491	6.097	5.876	-14.563	-13.115
	Zn site (1)	48.293*	75.277	5.419	5.440	-7.853	-23.158
	average over Cu and Zn atoms	29.765	47.333	5.876	5.699	-23.742	-19.198

^aAverage values are computed using the number of coordination sites (given in brackets) as weights.

values of reaction energies RE₁ and RE₂ for the first and second reactions, respectively. Moreover, the order of average reaction energies for both the reactions in Table 4 was found to be Cu₇ZnO < Cu₇Zn < Cu₈ < (Without a Catalyst). Note that the variation of reaction energies with the choice of the catalyst cluster should not be interpreted as a change in the equilibrium constant, as apart from the reactant(s) and product(s), the energy of the clusters is also included in their calculation. In this case, one of the reasons for more negative reaction energies for Cu₇Zn and Cu₇ZnO clusters compared to the Cu₈ cluster is the highly negative reaction energies for Zn sites. The average rate constants k_1 and k_2 in Table 4 follow the order Cu₈ < Cu₇ZnO < Cu₇Zn.

E_a depends strongly on the coordination for Cu sites. For the Cu₈ cluster, E_a values for both the reactions are much lower for the 5Co site compared to the 4Co site. The same trend is observed when comparing 5Co_Near and 4Co_Near or 5Co_Away and 4Co_Away sites for the Cu₇ZnO cluster. Similarly, E_a values for both the reactions on the 5Co_Away site of the Cu₇Zn cluster are lower than those of the 4Co_Away site. However, this general trend is not followed for the 5Co_Near site of the Cu₇Zn cluster, which has a higher activation barrier compared to the 4Co_Near site. The lowest E_a values (among all coordination sites of all clusters studied) were found for the 4Co_Near site of the Cu₇Zn cluster for the first reaction and the 5Co_Away site of the Cu₇Zn cluster for the second reaction. Also considering the previous conclusion regarding the average rate constants, we may therefore conclude that Cu₇Zn has the highest catalytic activity among the clusters studied.

4. CONCLUSIONS

In summary, we have performed detailed DFT calculations to analyze the glycerol hydrogenolysis reactions with Cu, Cu–Zn, and Cu–ZnO clusters. The main findings of this study may be summarized as follows:

- Glycerol to 1,2-PDO conversion is the most preferred hydrogenolysis route when using Cu-based catalysts, as

established by the comparison of activation barriers of different reaction pathways.

- 1-Propanol is a more preferred over-hydrogenolysis product of 1,2-PDO when using Cu-based catalysts, in comparison to methanol and ethanol or 2-propanol.
- Hydrogen and water molecules are not adsorbed on the catalyst surface during the glycerol hydrogenolysis reaction.
- ZnO doping promotes stronger adsorption of glycerol, 2-acetol, and 1,2-PDO in Cu catalysts.
- Extremely low rate constants and high activation barriers were found for the glycerol to 1,2-PDO reaction without the catalyst clusters, which establishes that the reactions are not feasible without a catalyst.
- Activation barriers depend strongly on the coordination for Cu sites. When averaged over all possible coordination sites, Cu₇Zn has the highest catalytic activity among the clusters studied.

Although the findings of this study appear to be quite conclusive, some of the drawbacks of the computational method adopted here require further deliberation. First, the catalyst clusters containing three and eight atoms used here for computational convenience are not the true representation of the bulk catalysts used in experimental studies on glycerol hydrogenolysis. Second, the effects of variations in Zn/ZnO doping are not considered. Third, experimental studies typically have catalysts supported on a surface (e.g., MgO), which is not considered in the model. Despite these obvious shortcomings, the fact that such simple cluster models are able to confirm some of the experimental findings and that these calculations are relatively easier to perform provides confidence in the possible use of these models in the computational screening of catalysts.

AUTHOR INFORMATION

Corresponding Author

Prateek K. Jha – Department of Chemical Engineering, IIT Roorkee, Roorkee, Uttarakhand 247667, India; orcid.org/0000-0001-9844-2875; Email: prateek.jha@ch.iitr.ac.in

Authors

Ram Singh – Department of Chemical Engineering, IIT Roorkee, Roorkee, Uttarakhand 247667, India

Prakash Biswas – Department of Chemical Engineering, IIT Roorkee, Roorkee, Uttarakhand 247667, India

Complete contact information is available at:

<https://pubs.acs.org/10.1021/acsomega.2c05342>

Notes

The authors declare no competing financial interest.

ACKNOWLEDGMENTS

P.K.J. acknowledges the INSPIRE award from the Department of Science and Technology (DST), India (no. IFA14/ENG-72).

REFERENCES

- (1) Bagheri, S.; Julkapli, N. M.; Yehye, W. A. Catalytic Conversion of Biodiesel Derived Raw Glycerol to Value Added Products. *Renewable Sustainable Energy Rev.* **2015**, *113*, 113–127.
- (2) Quispe, C. A. G.; Coronado, C. J. R.; Carvalho, J. A. Glycerol: Production, Consumption, Prices, Characterization and New Trends in Combustion. *Renewable Sustainable Energy Rev.* **2013**, *475*–493.
- (3) Nakagawa, Y.; Tomishige, K. Heterogeneous Catalysis of the Glycerol Hydrogenolysis. *Catal. Sci. Technol.* **2011**, *1*, 179–190.
- (4) Chaminand, J.; Djakovitch, L. A.; Gallezot, P.; Marion, P.; Pinel, C.; Rosier, C. Glycerol Hydrogenolysis on Heterogeneous Catalysts. *Green Chem.* **2004**, *6*, 359–361.
- (5) Dasari, M. A.; Kiatsimkul, P. P.; Sutterlin, W. R.; Suppes, G. J. Low-Pressure Hydrogenolysis of Glycerol to Propylene Glycol. *Appl. Catal., A* **2005**, *281*, 225–231.
- (6) Perosa, A.; Tundo, P. Selective Hydrogenolysis of Glycerol with Raney Nickel. *Ind. Eng. Chem. Res.* **2005**, *44*, 8535–8537.
- (7) Pudi, S. M.; Biswas, P.; Kumar, S. Selective Hydrogenolysis of Glycerol to 1,2-Propanediol over Highly Active Copper-Magnesia Catalysts: Reaction Parameter, Catalyst Stability and Mechanism Study. *J. Chem. Technol. Biotechnol.* **2016**, *91*, 2063–2075.
- (8) Pudi, S. M.; Biswas, P.; Kumar, S.; Sarkar, B. Selective Hydrogenolysis of Glycerol to 1,2-Propanediol over Bimetallic Cu-Ni Catalysts Supported on γ -Al₂O₃. *J. Braz. Chem. Soc.* **2015**, *26*, 1551–1564.
- (9) Wang, Y.; Zhou, J.; Guo, X. Catalytic Hydrogenolysis of Glycerol to Propanediols: A Review. *RSC Adv.* **2015**, *74611*–74628.
- (10) Zhao, H.; Zheng, L.; Li, X.; Chen, P.; Hou, Z. Hydrogenolysis of Glycerol to 1,2-Propanediol over Cu-Based Catalysts: A Short Review. *Catal. Today* **2020**, *84*–95.
- (11) Chiu, C. W.; Dasari, M. A.; Sutterlin, W. R.; Suppes, G. J. Removal of Residual Catalyst from Simulated Biodiesel's Crude Glycerol for Glycerol Hydrogenolysis to Propylene Glycol. *Ind. Eng. Chem. Res.* **2006**, *45*, 791–795.
- (12) Montassier, C.; Dumas, J. M.; Granger, P.; Barbier, J. Deactivation of Supported Copper Based Catalysts during Polyol Conversion in Aqueous Phase. *Top. Catal.* **1995**, *121*, 231–244.
- (13) Mondal, S.; Arifa, A. A.; Biswas, P. Production of 1,2-Propanediol from Renewable Glycerol Over Highly Stable and Efficient Cu–Zn(4:1)/MgO Catalyst. *Catal. Lett.* **2017**, *147*, 2783–2798.
- (14) Pandey, D. K.; Biswas, P. Production of Propylene Glycol (1,2-Propanediol) by the Hydrogenolysis of Glycerol in a Fixed-Bed Downflow Tubular Reactor over a Highly Effective Cu-Zn Bifunctional Catalyst: Effect of an Acidic/Basic Support. *New J. Chem.* **2019**, *43*, 10073–10086.
- (15) Xia, S.; Nie, R.; Lu, X.; Wang, L.; Chen, P.; Hou, Z. Hydrogenolysis of Glycerol over Cu_{0.4}/Zn_{5.6}-XMg_xAl₂O_{8.6} Catalysts: The Role of Basicity and Hydrogen Spillover. *J. Catal.* **2012**, *296*, 1–11.
- (16) Wang, S.; Liu, H. Selective Hydrogenolysis of Glycerol to Propylene Glycol on Cu-ZnO Catalysts. *Catal. Lett.* **2007**, *117*, 62–67.
- (17) Zhou, Z.; Li, X.; Zeng, T.; Hong, W.; Cheng, Z.; Yuan, W. Kinetics of Hydrogenolysis of Glycerol to Propylene Glycol over Cu-ZnO-Al₂O₃ Catalysts. *Chin. J. Chem. Eng.* **2010**, *18*, 384–390.
- (18) Hirunsit, P.; Luadthong, C.; Faungnawakij, K. Effect of Alumina Hydroxylation on Glycerol Hydrogenolysis to 1,2-Propanediol over Cu/Al₂O₃: Combined Experiment and DFT Investigation. *RSC Adv.* **2015**, *5*, 11188–11197.
- (19) Nimlos, M. R.; Blanksby, S. J.; Qian, X.; Himmel, M. E.; Johnson, D. K. Mechanisms of Glycerol Dehydration. *J. Phys. Chem. A* **2006**, *110*, 6145–6156.
- (20) Geng, Z.; Zhang, M.; Yu, Y. Theoretical Investigation on Pyrolysis Mechanism of Glycerol. *Fuel* **2012**, *93*, 92–98.
- (21) Laino, T.; Tuma, C.; Curioni, A.; Jochnowitz, E.; Stolz, S. A Revisited Picture of the Mechanism of Glycerol Dehydration. *J. Phys. Chem. A* **2011**, *115*, 3592–3595.
- (22) Karim, N. A.; Alias, M. S.; Kamarudin, S. K. The Mechanism of the Water Dissociation and Dehydrogenation of Glycerol on Au (111) and PdAu Alloy Catalyst Surfaces. *Int. J. Hydrogen Energy* **2021**, *46*, 30937–30947.
- (23) Guan, J.; Wang, X.; Wang, X.; Mu, X. Thermodynamics of Glycerol Hydrogenolysis to Propanediols over Supported Copper Clusters: Insights from First-Principles Study. *Sci. China Chem.* **2013**, *56*, 763–772.
- (24) Chen, Y.; Saliccioli, M.; Vlachos, D. G. An Efficient Reaction Pathway Search Method Applied to the Decomposition of Glycerol on Platinum. *J. Phys. Chem. C* **2011**, *115*, 18707–18720.
- (25) Singh, R.; Biswas, P.; Jha, P. K. Density Functional Theory Investigation of Structure, Stability, and Glycerol/Hydrogen Adsorption on Cu, Cu-Zn, and Cu-ZnO Clusters. *Int. J. Quantum Chem.* **2020**, *120*, No. e26239.
- (26) Frisch, M. J.; Trucks, G. W.; Schlegel, H. B.; Scuseria, G. E.; Robb, M. A.; Cheeseman, J. R.; Scalmani, G.; Barone, V.; Mennucci, B.; Petersson, G. A.; et al. *Gaussian 09*, revision D.01; Gaussian Inc.: Wallingford, CT, 2013.
- (27) Becke, A. D. Density-Functional Thermochemistry. III. The Role of Exact Exchange. *J. Chem. Phys.* **1993**, *98*, 5648–5652.
- (28) Hay, P. J.; Wadt, W. R. *Ab Initio* Effective Core Potentials for Molecular Calculations. Potentials for K to Au Including the Outermost Core Orbitals. *J. Chem. Phys.* **1985**, *82*, 299–310.
- (29) Wadt, W. R.; Hay, P. J. *Ab Initio* Effective Core Potentials for Molecular Calculations. Potentials for Main Group Elements Na to Bi. *J. Chem. Phys.* **1985**, *82*, 284–298.
- (30) Hay, P. J.; Wadt, W. R. *Ab Initio* Effective Core Potentials for Molecular Calculations. Potentials for the Transition Metal Atoms Sc to Hg. *J. Chem. Phys.* **1985**, *82*, 270–283.
- (31) Fukui, K. A Formulation of the Reaction Coordinate. *J. Phys. Chem. A* **1970**, *74*, 4161–4163.
- (32) Eyring, H. The Activated Complex in Chemical Reactions. *J. Chem. Phys.* **1935**, *3*, 63–71.
- (33) Evans, M. G.; Polanyi, M. Some Applications of the Transition State Method to the Calculation of Reaction Velocities, Especially in Solution. *Trans. Faraday Soc.* **1935**, *31*, 875–894.